

## OPTICAL PROPERTIES OF THIN Cu FILMS AS A FUNCTION OF SUBSTRATE TEMPERATURE

H. Savaloni<sup>1,\*</sup> and A.R. Khakpour<sup>2</sup>

<sup>1</sup> *Department of Physics, Faculty of Sciences, University of Tehran, North-Kargar  
Street, Tehran, Islamic Republic of Iran*

<sup>2</sup> *Iranian Aerospace Organization, Fajre Industrial Group, Tehran, Islamic Republic of Iran*

### Abstract

Copper films (250 nm) deposited on glass substrates, at different substrate temperatures. Their optical properties were measured by ellipsometry (single wavelength of 589.3 nm) and spectrophotometry in the spectral range of 200–2600 nm. Kramers Kronig method was used for the analysis of the reflectivity curves of Cu films to obtain the optical constants of the films, while ellipsometry measurement was carried out as an independent method. The influence of substrate temperature on the microstructure of thin metallic films [Structure Zone Model (SZM)] is well established. The Effective Medium Approximation (EMA) analysis was used to establish the relationship between the SZM and EMA predictions. Good agreements between SZM as a function of substrate temperature and the values of volume fraction of voids obtained from EMA analysis, are obtained; by increasing the substrate temperature the separation of the metallic grains decreases hence the volume fraction of voids decreases and denser films are formed. The unusual (anomalous) behavior of the void fraction as a function of wavelength for different substrate temperatures, in certain wavelength region is explained to be due to the roughness value of the film surface. This value corresponds to this wavelength region scattering from the surface roughness. This phenomenon may be used as a technique for surface roughness measurement.

**Keywords:** Structure Zone Model (SZM); Effective Medium Approximation (EMA); Optical functions; Substrate temperature; Surface roughness

### 1. Introduction

The growth of thin metal films and the relation of their different properties with growth conditions has

become subject of great interest to those using physical vapor-deposition processes. The reason is that their structure and related properties can be modified and controlled as a function of substrate temperature,

---

\* E-mail: savaloni@molavi.ut.ac.ir

deposition rate and other parameters [1].

The influence of different deposition parameters on the structure of metallic films has been reported by many researchers [2-8].

On the other hand, the influence of substrate temperature, for example, on the optical properties of discontinuous silver and Aluminum and gold thin films has been reported by Ward [9] and Dobierzewska-Mozrzymas *et al.* [10,11], Maxwell-Garnett was the first to give a model for optical constants of discontinuous thin films, which was based on the dispersion of light from uniformly distributed small spherical particles on the substrate surface. Hunderi [12] suggested a simple theory for the influence of grain boundaries and lattice defects on optical constants of Au, Ag, Na and K thin films.

The other model for obtaining the effective dielectric function of a grain, is the effective medium theory [13]. In this model the film is considered as a two phase arrangement (*e.g.*, as a combination of deposited material and the vacuum or a combination of two materials deposited).

Aspenes [14], also reported a simple model for determination of optical constants of non-uniform media, which is in fact considered as a mixture of segregated regions of two or more materials, while each of them retain their original dielectric properties. For example, polycrystalline films (*e.g.*, metallic thin films) which are a non-uniform combination of the film material and voids, can be considered. In special cases, one can re-produce both Maxwell-Garnett [15,16], and Bruggmann [13] theories. Aspenes [14] gives the following equation for the two phases effective medium

$$\frac{\varepsilon' - \varepsilon_h}{\varepsilon' + 2\varepsilon_h} = f_a \frac{\varepsilon_a - \varepsilon_h}{\varepsilon_a + 2\varepsilon_h} + f_b \frac{\varepsilon_b - \varepsilon_h}{\varepsilon_b + \varepsilon_h} \quad (1)$$

In which  $\varepsilon_a$ ,  $\varepsilon_b$ ,  $f_a$  and  $f_b$  are dielectric constants and volume fractions of the phases a and b, respectively, and  $\varepsilon_h$  is the host dielectric constant. Specifically, if b represents the dilute phase then we should choose  $\varepsilon_h = \varepsilon_a$ , so:

$$\frac{\varepsilon - \varepsilon_a}{\varepsilon + 2\varepsilon_a} = f_b \frac{\varepsilon_b - \varepsilon_a}{\varepsilon_b + 2\varepsilon_a} \quad (2)$$

Equation (2) and the alternative equation with  $\varepsilon_h = \varepsilon_b$ , are the Maxwell Garnett effective medium expressions [15,16]. In case where  $f_a$  and  $f_b$  are comparable, it may not be clear whether a or b is the host medium. One alternative way is simply to make the self-consistent choice  $\varepsilon_h = \varepsilon$ , so Equation (1) reduces to

$$0 = \frac{\varepsilon_a - \varepsilon}{\varepsilon + 2\varepsilon} + f_b \frac{\varepsilon_b - \varepsilon}{\varepsilon_b + 2\varepsilon} \quad (3)$$

Parmigiani *et al.* [17] studied optical and electrical properties of thin silver films (50 nm, an optical thickness to support surface plasmons) grown under ion bombardment. They obtained reflectivity curves by attenuated total reflection in the Kretschmann [18] configuration on the base of a glass prism [19]. A comparative study between their optical data and the measured strain, grain size, and lattice parameter suggested that the differences in dielectric function between the bulk metal and the ion-bombarded film arise mainly from the presence of voids and changes in grain size. The fraction of voids was determined from the dielectric function for a homogeneous sample of silver, their measured values of the dielectric function in the bombarded films and the Bruggeman effective-media approximation (EMA).

It is well known that grain size in thin metallic films increases with the substrate temperature [4-6]. Hence, the grain boundaries change, due to diffusion processes. Both the mobility and the activation energy for the migration of a grain boundary depend on its crystallography [20]. Accordingly, at any given temperature, boundaries with different crystallography will migrate at different rates, and the lower the temperature the smaller the proportion of mobile boundary types. Grovenor *et al.* [7] suggest that three regimes of film growth, corresponding to increasing  $T_s$ , can be distinguished phenomenologically according to whether (a) one or fewer, (b) two, or (c) all the boundaries of grain are mobile. Therefore it is of interest to find out the relationship between different theories [13,14,21] given for optical parameters and the structural changes described by variation of substrate temperature (Structure Zone Model, SZM) [2-8]. Accordingly, it was decided to investigate the influence of substrate temperature on the optical properties of Cu films.

## 2. Experimental Details

Copper (fcc) films of 250 nm thickness with a deposition rate of about  $0.5 \text{ nm s}^{-1}$  were produced by resistive evaporation from Mo boats. The purity of copper was 99.99+%. A (Veeco VES770) coating plant with a base pressure of  $10^{-6}$  Torr was used. The pressure during evaporation was typically about  $10^{-5}$  Torr. In order to keep the evaporation condition for all substrates and temperatures constant [4], a substrate system with a solar system configuration was designed and constructed. In this system, six substrate holders

(planets) were able to move on six arms from the center of the system, providing positions for different angles of incidence, and rotate around cylinder axis and the main (solar) system axis, providing uniform deposition. In this work the rotation facility of the system was not used. Each substrate holder was heated, using a thermal filament wrapped on a cylindrical ceramic with 12 grooves and encapsulated inside a stainless steel cylinder and was mounted on the cylinder axis. This cylinder was closed at one base and on its other base the copper substrate holder was fitted on the cylinder axis. In order to insulate the inner surface of the cylinder, electrically and its outer surface thermally, ZrO<sub>2</sub> and Al<sub>2</sub>O<sub>3</sub> thick coatings were used, respectively. ZrO<sub>2</sub> and Al<sub>2</sub>O<sub>3</sub> were spray coated on the inner and the outer surfaces of the stainless steel cylinder. On each copper disk substrate holder the substrate (a disk of 25mm diameter and 1.0 mm thickness glass cut from microscope slides, or 22 mm × 22 mm × 0.15 mm thick glass cover slips) can be fixed by a stainless steel mask. The substrate temperatures were controlled by programmed thermostats and thermocouples fixed inside a hole on the surface of copper disk substrate holder.

Just before use, all glass substrates were ultrasonically cleaned in heated acetone then ethanol. The surface texture of the substrates was measured by a Talystep or a Talysurf profilometer. The rms substrate roughness R<sub>q</sub> for glass was 0.3 nm. The substrate positions were chosen, so that their normal to the direction of incidence of the evaporant beam was at 18° and the distance between the center of the evaporation boat and the center of the substrate holder system was 15.2 cm. In order to provide a point source for geometrical reasons, a plate of Mo with a 6 mm diameter hole in the middle was used as a mask (cap) on top of the evaporation boat. In this way, six films can be produced at 6 different substrate temperatures, under the same evaporation condition, in one evaporation run. The deposition process was repeated several times and reproducibility of the results was confirmed. Film thickness was measured using the RBS technique, which also provided us with an estimation of film density. The near normal incidence reflectance spectra are obtained using a double beam spectrophotometer (Carry 500 Scan) in the spectral range of (200-2600 nm) corresponding to the energy range of (0.415-6.15 eV). A fixed wavelength (λ = 589.3 nm) ellipsometer is also used for ellipsometric measurements, as an independent method.

### 3. Physics of Dielectric Functions

The real and imaginary parts of the refractive index  $\tilde{n} = n + ik$  of a material are given by the expressions:

$$\frac{(n - 1 - ik)}{(n + 1 - ik)} = R^{1/2} e^{i\theta} \tag{4}$$

$$\epsilon = \epsilon_1 - i\epsilon_2 = (n + ik)^2 \tag{5}$$

$$\epsilon_1 = n^2 - k^2 \tag{6}$$

$$\epsilon_2 = 2nk \tag{7}$$

where R is the normal incidence reflectance and θ is the phase angle used in expressing the complex reflectivity r in polar form,

$$r(\omega) = R^{1/2}(\omega) e^{i\theta(\omega)}. \tag{8}$$

The phase angle θ(E<sub>0</sub>) at energy E<sub>0</sub> can be calculated rigorously from the Kramers–Kronig (K-K) integral

$$\theta(E) = \frac{E}{\pi} \int_0^\infty \frac{\ln[R(E)/R(E_0)]}{E^2 - E_0^2} dE \tag{9}$$

where E is the photon energy, provided that the reflectance R(E) is known for all energies.

However, since R is not known over the entire energy spectrum, it is necessary to extrapolate R(E) to infinite energies, usually by a power law. One can use an extrapolation which will force the optical or dielectric constants to agree with some independent measurement at a particular energy. For example, ellipsometric measurements on metals will yield ε<sub>1</sub>, ε<sub>2</sub> or n, k directly.

In order to calculate θ(ω) from Equation (9) the following procedure can be adopted. At very low energies we assume that the reflectance at zero energy approaches unity. At high energies, when the incident photon energy is higher than a certain energy E<sub>2</sub> (which is about 30 eV for Cu), the reflectance is determined from free electron asymptotic limit [22]

$$R(E) = R(E_2) \left(\frac{E}{E_2}\right)^{-4} \quad E > E_2 \tag{10}$$

substituting Equation (10) in K-K Equation (9), yields

$$\begin{aligned} \theta(E) = & -\frac{E}{\pi} \int_0^{E_2} \frac{\ln R(E) - \ln R(E_0)}{E^2 - E_0^2} dE \\ & + \frac{1}{2\pi} \ln \left[ \frac{R(E)}{R(E_2)} \right] \ln \left| \frac{E_2 + E}{E_2 - E} \right| \\ & + \frac{1}{\pi} \sum_{n=0}^\infty \left[ 4 \left( \frac{E}{E_2} \right)^{2n+1} \right] (2n + 1) \end{aligned} \tag{11}$$

hence, if  $E_2$  is known, the  $\theta(E)$  can be calculated. If the film thickness is taken as a known parameter, then for calculation of the real and the imaginary parts of the refractive index of the layer (thin film) ( $n_2$ ,  $k_2$ ), two equations at one frequency are required. By substituting the known values of  $\theta(E)$  and  $R(E)$  in Equation (8) the reflectance index  $r(E)$  can also be determined with reference to the reflectance equation for a thin film [9], as:

$$r = \frac{r_{12} + r_{23} \exp(2i\delta_2) + r_{31} \exp[2i(\delta_2 + \delta_3)] + r_{12} r_{23} r_{31} \exp(2i\delta_3)}{1 + r_{12} r_{23} \exp(2i\delta_2) + r_{12} r_{31} \exp[2i(\delta_2 + \delta_3)] + r_{23} r_{31} \exp(2i\delta_3)} \quad (12)$$

where  $r_{12}$ ,  $r_{23}$ ,  $r_{31}$ ,  $t_{12}$ ,  $t_{23}$ , and  $t_{31}$  are Fresnel reflectance and transmittance indices for air-film, film-substrate and substrate-air boundaries, respectively, and

$$r_{12s,p} = \frac{\pm 1 \mp (n_2 + ik_2)}{1 + (n_2 + ik_2)} \quad (13a)$$

$$r_{23s,p} = \frac{\pm (n_2 + ik_2) \mp n_s}{(n_2 + ik_2) + n_s} \quad (13b)$$

$$r_{31s,p} = \frac{\pm n_s \mp 1}{n_s + 1} \quad (13c)$$

$$\delta_2 = \frac{Ed_2}{\hbar c} (n_2 + ik_2) \quad (13d)$$

$$\delta_3 = \frac{Ed_3}{\hbar c} n_3 \quad (13e)$$

where  $d_2$  and  $d_3$  are the film and the substrate thicknesses, respectively. In the case of normal incidence we have;

$$R^{\frac{1}{2}}(E)_{\text{exp}} \cos \theta(E)_{\text{exp}} - \text{Re}[\Gamma(n_2(E), k_2(E), d_2)] = 0 \quad (14-a)$$

$$R^{\frac{1}{2}}(E)_{\text{exp}} \sin \theta(E)_{\text{exp}} - \text{Im}[\Gamma(n_2(E), k_2(E), d_2)] = 0 \quad (14-b)$$

when the real and imaginary parts of the refractive index are determined, we can calculate the absorption coefficient as;

$$\alpha(E) = \frac{2E}{\hbar c} k_2(E) \quad (15)$$

and dielectric function using equations (5)–(7).

In obtaining equations 14(a) and 14(b) from equation

(12) no approximation was applied, this makes the task very complicated even for normal incidence. Most researchers use variety of approximations, which the most popular one is infinite substrate approximation [23]. Application of this approximation causes the omission of the third and the fourth terms in both nominator and denominator in equation (12).

As mentioned before when  $R$  is not known over the entire energy range, one must extrapolate  $R(E)$  to infinite energy. Since our experimental measurements is limited to the energy range (0.4–6.15 eV), we were forced to use some available data on the remaining energy range, namely (6.15–30 eV). Hagemann [24] has reported some data on Cu films produced at room temperature. Hence we normalized our lowest temperature results ( $T_s = 368$  K) to that of Hagemann and applied this procedure to higher temperature films too. In this way we can calculate optical functions of our films by the Kramers-Kronig method.

However, as an independent measurement, the ellipsometric method with fixed ( $\lambda = 589.3$  nm) wavelength was used, and the results of  $\epsilon_1$ ,  $\epsilon_2$ ,  $n$  and  $k$  of this method showed very good agreement with those of K-K method at the same wavelength. Therefore, we may expect that the generalization of the results over the whole range of wavelength examined is valid.

## 4. Results

### 4.1. Ellipsometry

As mentioned above the ellipsometry method was used as an independent check on K-K method. The results of ellipsometry measurements are summarized for Cu/glass films of varying substrate temperatures in Table 1.

Table 1 and Figure 1(a-d) show the variations of  $n$ ,  $k$ ,  $\epsilon_1$  and  $\epsilon_2$  with substrate temperature for Cu/glass films. It can be seen that by increasing the substrate temperature,  $k$  and  $\epsilon_2$  increase while  $\epsilon_1$  decreases and ultimately all three parameters reach an asymptotic value (constant value) (at temperatures higher than a certain value (~600 K)). The reason for this type of variation is due to the fact that with increasing the substrate temperature, thermal diffusion process increases. Hence the voids in the microstructure of the growing film decrease, resulting in higher density films, until the film reaches its highest density, and its density no longer increases. In Table 1 the increase in absorption coefficient for Cu films confirms this suggestion. Therefore according to Aspnes' [21] effective medium theory, this process causes an increase

**Table 1.** Optical constants of Cu/glass films produced at different  $T_s$ , substrate thickness = 0.16 mm, obtained from ellipsometry method ( $\lambda = 589.3$  nm) measurements.  $\gamma$  and  $\Delta$  are the ellipsometric angles,  $\alpha$  is the absorption coefficient

Samples Zone II $d = 260 \pm 2.5$ nm	$\gamma \pm 3.6 \times 10^{-5}$ $\Delta \pm 7.6 \times 10^{-2}$ (rad)	$n \pm 0.01$ $k \pm 0.1$	$\epsilon_1 \pm 0.55$ $\epsilon_2 \pm 0.15$	$\alpha \pm 1.05$ ( $\mu\text{m}^{-1}$ )
$T_s = 368 \pm 5\text{K}$ $T_s / T_m = 0.27$	<b>4.445</b> <b>1.147</b>	<b>0.513</b> <b>2.128</b>	<b>-4.265</b> <b>2.177</b>	23.648
$T_s = 388 \pm 5\text{K}$ $T_s / T_m = 0.28$	<b>4.14</b> <b>1.124</b>	<b>0.498</b> <b>2.251</b>	<b>-4.819</b> <b>2.242</b>	24.000
$T_s = 413 \pm 5\text{K}$ $T_s / T_m = 0.304$	<b>4.09</b> <b>1.11</b>	<b>0.501</b> <b>2.385</b>	<b>-5.437</b> <b>2.389</b>	25.429
$T_s = 433 \pm 5\text{K}$ $T_s / T_m = 0.32$	<b>4.09</b> <b>1.11</b>	<b>0.521</b> <b>2.457</b>	<b>-5.765</b> <b>2.560</b>	26.196
$T_s = 473 \pm 5\text{K}$ $T_s / T_m = 0.34$	<b>4.0</b> <b>1.1</b>	<b>0.524</b> <b>2.584</b>	<b>-6.402</b> <b>2.708</b>	27.551
$T_s = 503 \pm 5\text{K}$ $T_s / T_m = 0.37$	<b>3.92</b> <b>1.076</b>	<b>0.511</b> <b>2.721</b>	<b>-7.142</b> <b>2.781</b>	29.011

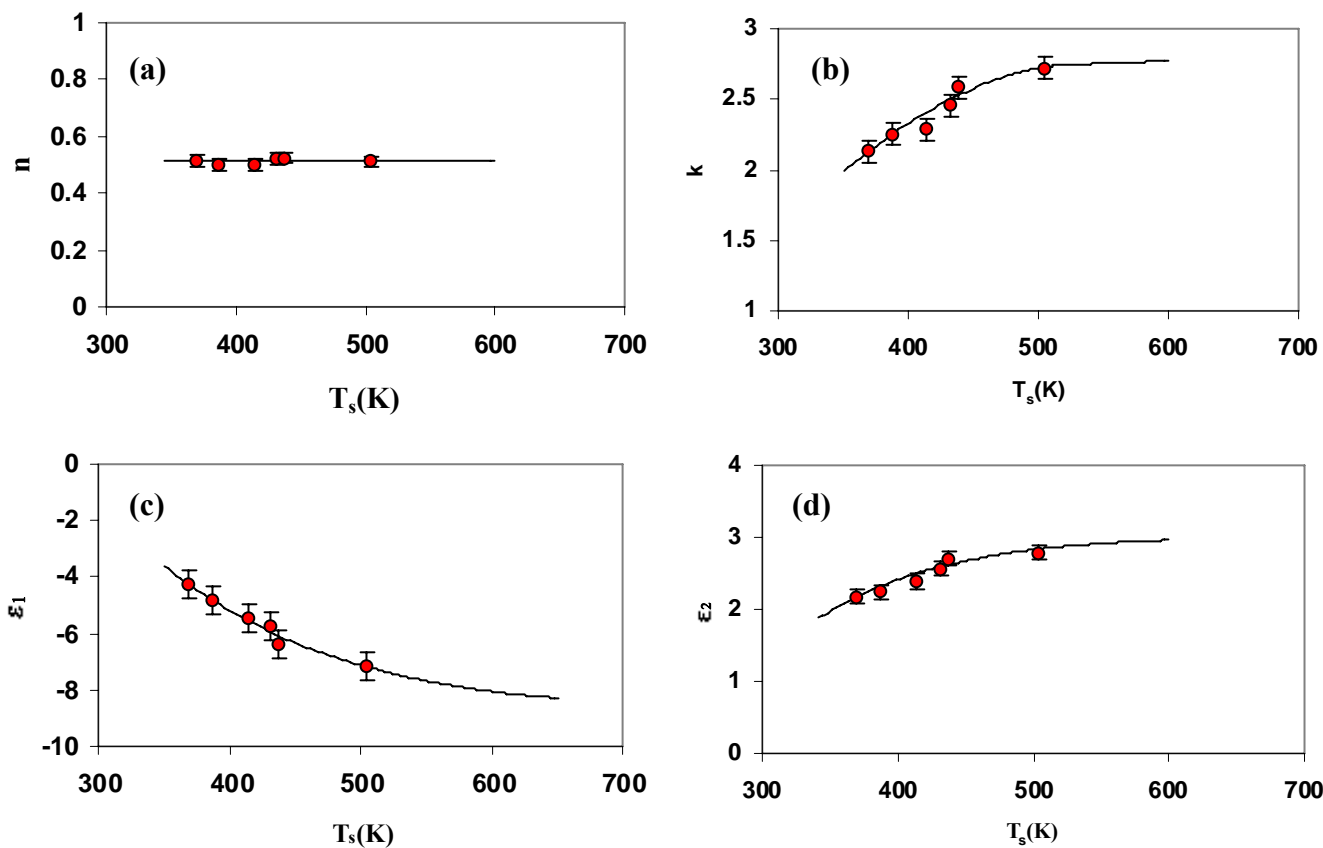


**Figure 1.** The optical functions of Cu/glass films for six different substrate temperatures obtained by ellipsometry. (a)  $n$ ; (b)  $k$ ; (c)  $\epsilon_1$ ; (d)  $\epsilon_2$ .

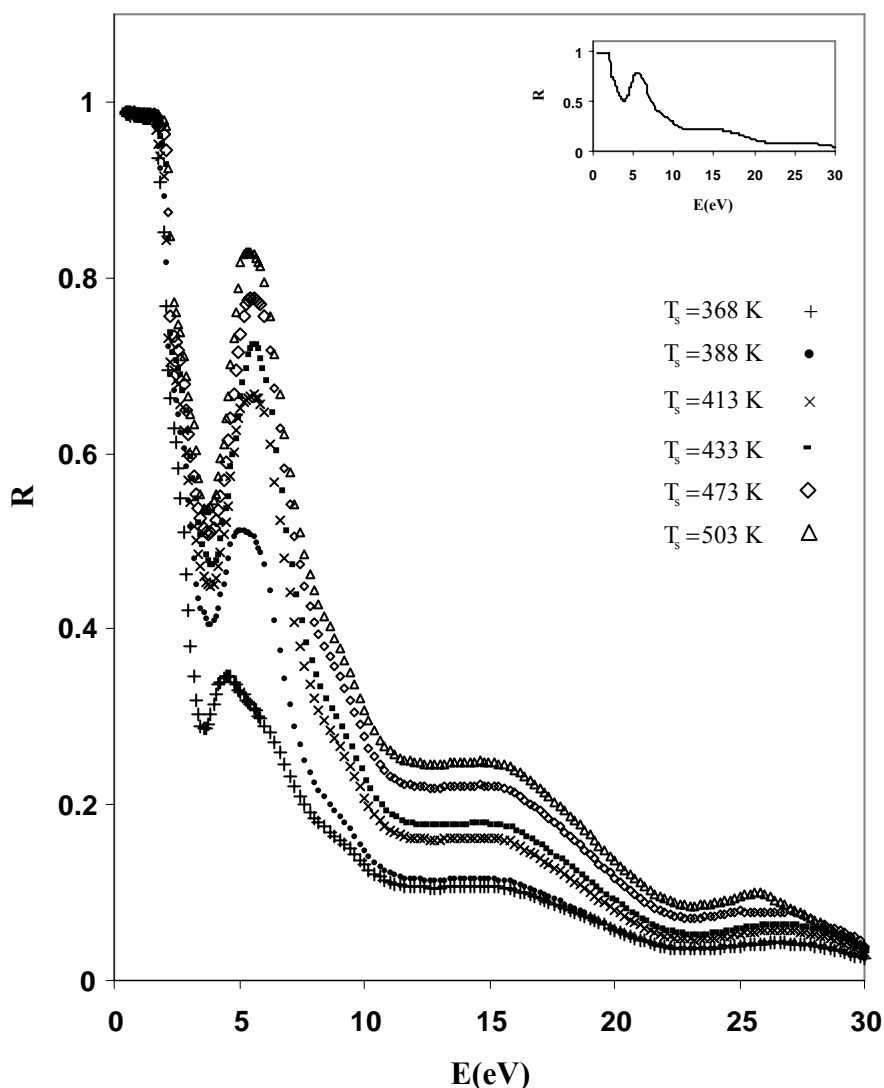


**Figure 2.** Reflectivity curves of Cu/glass films for six different substrate temperatures. Inset is the Hagemann's results [24].

in imaginary part of the dielectric function and a decrease in the real part of the dielectric function.

It can also be seen in Table 1 and Figure 1(a), that by increasing the substrate temperature the real part of refractive index,  $n$ , remains constant for Cu films, reflecting that,  $n$ , is independent of the substrate temperature.

#### 4.2. Kramers–Kronig Analysis

Figure 2 shows the reflectance spectra of Cu/glass films of varying substrate temperatures, using the normalization procedure to Hagemann's [24] results, described in Section 3. The inset shows Hagemann's

results for room temperature films. Our experimental results cover the energy range up to 6.15 eV. It is evident that over the higher energy range the variation of reflectance spectra is not pronounced, therefore the normalization procedure applied here cannot produce, even in the worst case, a significant deviation from the real value, while the independent method of ellipsometry has also proved a good agreement with the K-K results.

Figures 3(a-b) show the spectra for  $\epsilon_1$ , and  $\epsilon_2$  for Cu/glass films at different substrate temperatures ( $T_s$ ). The Hagemann's results are given in the insets. As in ellipsometry method (EM) the spectra of  $n$  for different

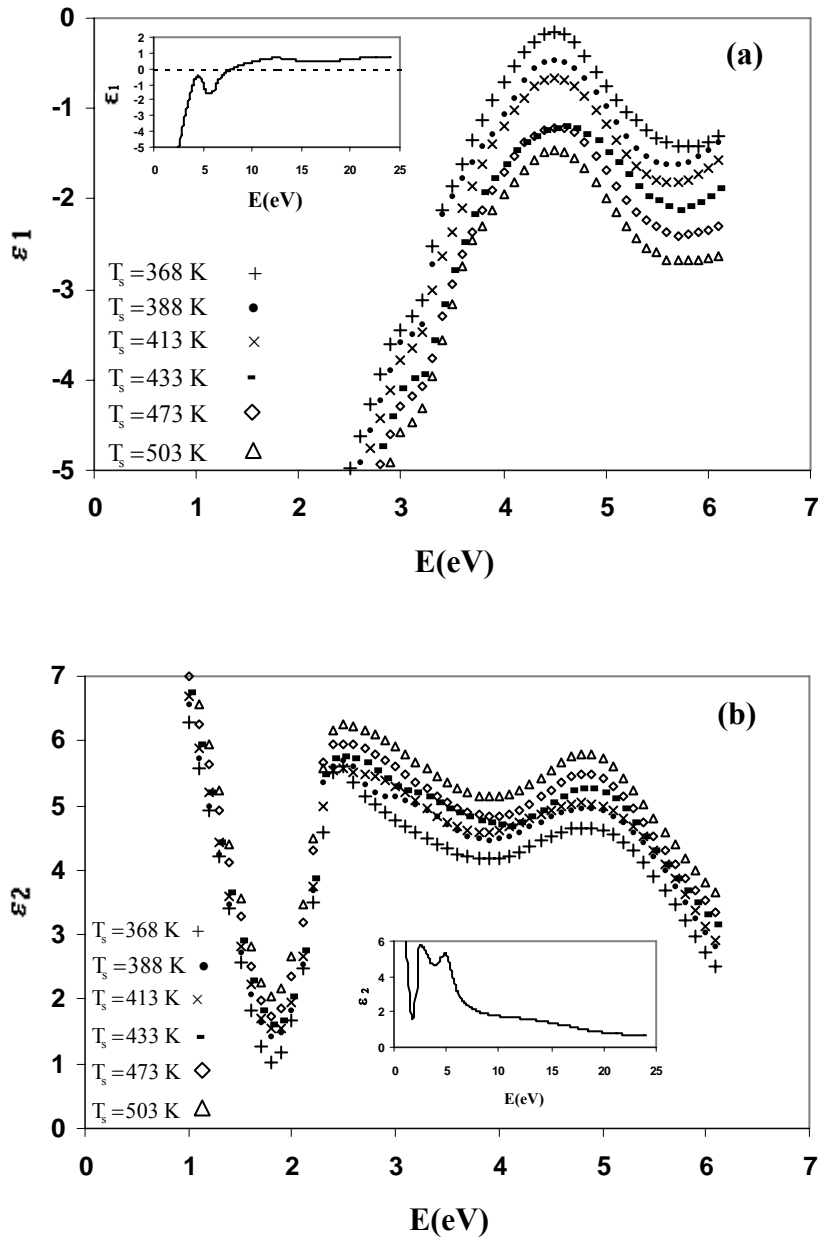


**Figure 3.** The dielectric constants of Cu/glass films for six different substrate temperatures. (a) Real part; (b) Imaginary Part.

$T_s$  did not vary with  $T_s$ , and agree well with both (EM) and Aspnes's effective medium theory. In the same manner as (EM) results,  $\epsilon_2$  and  $k$  increase with  $T_s$  while  $\epsilon_1$  decreases with  $T_s$  for Cu/glass, confirming the results given in Section (4-1).

### 5. Discussion; Effective Medium Approximation (EMA)

The fraction of voids can be computed from the Bruggeman effective medium approximation (EMA) [13]. Aspnes [21] gives the following equation for the effective dielectric function,  $\langle \epsilon \rangle$ , of heterogeneous

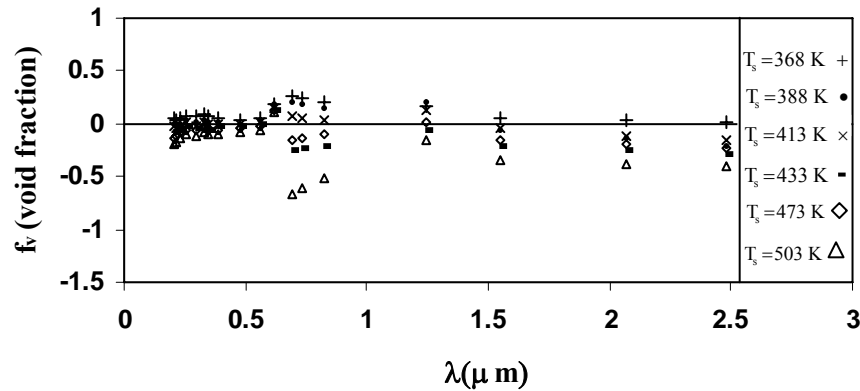


Figure 4. Void fraction vs. wavelength for different substrate temperatures.

material containing a volume fraction,  $f_v$  of voids as:

$$\frac{\langle \varepsilon \rangle - \varepsilon_h}{\langle \varepsilon \rangle + 2\varepsilon_h} = f_v \frac{1 - \varepsilon_h}{1 + 2\varepsilon_h} + (1 - f_v) \frac{\varepsilon - \varepsilon_h}{1 + 2\varepsilon_h}. \quad (16)$$

In Equation (16) if we take ( $\varepsilon_h = \langle \varepsilon \rangle$ ) the EMA can be obtained, which treats both void and material phases on equal, self-consistent basis. We have

$$f_v \left[ \frac{1 - \varepsilon_h}{1 + 2\varepsilon_h} \right] = (f_v - 1) \left[ \frac{\varepsilon - \varepsilon_h}{\varepsilon + 2\varepsilon_h} \right]. \quad (17)$$

Using Equation (17) in which  $\varepsilon$  is the value for bulk metal, the fraction of voids for each film over the whole measured energy range of (0.4 – 6.15 eV) was obtained by least square fit to Equation (17).

The results for Cu/glass films with six different substrate temperatures are given in Figure 4. As expected from the Structure Zone Model (SZM) [2,3] predictions, the fraction of voids decreases with increasing substrate temperature, confirming the discussion presented in section 1; as the substrate temperature increases, the grain size and the film density increases, while the void fraction in the film decreases. In Figure 4, it can be seen that for short wavelength region ( $<1.5 \mu\text{m}$ ) and at lower temperatures (*i.e.*  $\leq 413\text{K}$ ) the density of the films is less than bulk (positive values for  $f_v$ ;  $f_v = 0$  is taken as the value for the bulk) and at higher temperatures ( $\geq 473\text{K}$ ) it is more than bulk material (negative values for  $f_v$ ) as explained by Aspnes [21], with small variation over the wavelength range examined. It is usually expected that the void fraction  $f_v$  be independent of wavelength, as can be seen in the limited range of the wavelength (0.4416 – 0.6328  $\mu\text{m}$ ) in the report of Parmigiani *et al.* [17] (see Table 2

of reference [17]). However, our results cover a wide range of wavelength (0.2–2.6  $\mu\text{m}$ ) (Fig. 4) and show some variation (somewhat insignificant in most regions) in different wavelength regions. This phenomenon may be explained in the following way; copper films (250 nm) are not so thick to be considered as films with smooth surfaces. Generally, at this thickness, as our previous works [4-6,25] confirm (see for example, Figure 1 of reference [5] and Figures 2-4 of reference [25]), the films should contain well separated grains with valleys between them. Hence, in Cu films which are rough, the  $f_v$  variation should be almost independent of wavelength, as roughness is in such a size that all wavelengths go through similar process on incidence of light on the surface of the film (*i.e.* they do not see the roughness when the wavelength is larger than the roughness value). However at a particular wavelength (critical value) (0.65–0.85  $\mu\text{m}$ , in Figure 4) which may correspond to the roughness value, the scattering peaks up and the anomalous behavior in void fraction plot appears. In thicker films ( $\sim 1 \mu\text{m}$ ) we expect that, films be smoother and contain smaller peaks and valleys or holes at the tricorners of the neighboring grains [4-6,25]. Therefore, causing increased scattering at short wavelengths. One may suggest that, this phenomenon can be used as a measuring technique for surface roughness measurement. This, in fact is under further investigations and will be reported in the near future, particularly on Ag/glass films of  $\sim 1 \mu\text{m}$  thickness.

## 6. Conclusion

The aim of this work was to achieve a proper relationship between the microstructure of thin films as a function of substrate temperature (as discussed

thoroughly by many authors, including Savaloni and coworkers) and the optical properties of thin films. Therefore, Cu was selected for this study. The Kramers Kronig relation was employed for the analysis of the reflection spectra from the films, and very good agreement with ellipsometric measurements as an independent check on the results was obtained. The results for different substrate temperatures showed that the fraction of voids obtained, using EMA method agrees well with the prediction of SZM model; increasing the substrate temperature, increases the grain size through diffusion processes, hence reducing the void fraction in the film structure. An explanation for the different behavior of the void fraction with the wavelength, particularly at a critical wavelength region, based on the roughness of the films of different thicknesses is given. A suggestion is given, to the extent that, this anomalous behavior of void fraction versus wavelength, may be used as a roughness measurement technique for films and surfaces. More experimental work and analysis on this issue, are currently being carried out and will be reported in the near future.

#### Acknowledgement

This work was carried out with the support of the University of Tehran.

#### References

1. Macleod H.A. *In: Thin Film Optical Filters*. Adam Hilger Ltd, Bristol (1986).
2. Movchan B.A. and Demchishin A.V. *Phys. Met. Metall.*, **28**: 83 (1969).
3. Thornton J.A. *J. Vac. Sci. Technol.*, **12**: 830 (1975).
4. Savaloni H. and Bagheri Najmi S. *Vacuum*, **66**: 49 (2002).
5. Savaloni H. and Player M.A. *Ibid.*, **46**: 167 (1995).
6. Savaloni H., Player M.A., Gu E., and Marr G.V. *Ibid.*, **43**: 965 (1992).
7. Grovenor C.R.M., Hentzell H.T.G., and Smith D.A. *Acta Metall.*, **32**: 773 (1984).
8. Messier R. and Yehoda J.E. *J. Appl. Phys.*, **58**: 3739 (1985).
9. Ward L. *The Optical Constants of Bulk Materials and Films*. IOP Publishing Co., UK (1998).
10. Dobierzewska-Mozrzymas E., Peisert J., and Bieganski P. *Applied Optics*, **27**: 181 (1988).
11. Dobierzewska-Mozrzymas E., Peisert J., and Bieganski P. *Ibid.*, **24**: 727 (1985).
12. Hunderi O. *Phys. Rev.*, **B7**: 3419 (1973).
13. Bruggeman D.A.G. *Ann. Phys.*, (Leipzig), **24**: 636 (1935).
14. Aspnes D.E. *Thin Solid Films*, **89**: 249 (1982).
15. Maxwell Garnett J.C. *Philos. Trans. R. Soc. London*, **203**: 385 (1904).
16. Maxwell Garnett J. C. *Ibid.*, Ser. A. **205**: 237 (1906).
17. Parmigiani F., Key E., Huang T.C. Perrin J., Jurich M., and Swalen J.D. *Phys. Rev.*, **B23**: 879 (1986).
18. Kretschmann E. and Raether H. *Z. Naturforsch.*, **23**: 2135 (1968).
19. Guger H., Jurich M., Swalen J.D., and Sievers A.J. *Phys. Rev.*, **B30**: 4189 (1984).
20. Haessner F. and Hofmann S. *In: Haessner F. (Ed.), Recrystallization of Metallic Materials*. p 63. Dr Reider, Stuttgart (1978).
21. Aspnes D.E., Kinsbron E., and Bacon D.D. *Phys. Rev.*, **B21**: 3290 (1980).
22. Palik E.D. *Handbook of Optical Constants of Solids*. Courtesy Academic Press Inc (1985).
23. Alperovich L.I. and Pushkarev V.N. *Opt. Spectroscopy*, **47**: 5 (1979).
24. Hagemann H.J., Gudat, and Kunz G. *J. Opt. Soc. Am.*, **65**: 742 (1975).
25. Savaloni H. and Player M.A. *Thin Solid Films*, **256**: 48 (1995).